

**PRODUCTION OF  $3\pi^0$  IN  $pp$  REACTIONS ABOVE THE  $\eta$  PRODUCTION  
THRESHOLD AND THE QUADRATIC SLOPE PARAMETER  $\alpha$ <sup>1</sup>**

**C. Pauly<sup>2,a</sup>, L. Demirörs<sup>a</sup>, W. Scobel<sup>a</sup>**  
**for the CELSIUS-WASA collaboration**

<sup>a</sup>*Institut für Experimentalphysik der Universität Hamburg, D-22761 Hamburg, Germany*

Received 14 November 2005, in final form 11 January 2006, accepted 26 January 2006

The CELSIUS-WASA setup has been used to measure the production of  $3\pi^0$  in  $pp$  interactions at  $T_p = 1360$  and  $1450$  MeV. A cross section for the prompt  $pp \rightarrow pp3\pi^0$  and resonant  $pp \rightarrow pp(\eta \rightarrow 3\pi^0)$  reaction channel is determined. The efficiency corrected Dalitz plot and density distribution for the  $\eta \rightarrow 3\pi^0$  decay are shown, together with a fit of the quadratic slope parameter  $\alpha$ . Our preliminary result for  $\alpha$  is  $-0.027 \pm 0.009(stat) \pm 0.01(syst)$ .

PACS: 12.38.Bx, 13.25.Jx, 14.40.Aq, 25.40.Ve

## 1 Introduction

The  $\eta$  meson has a decay width of about 1.3 keV, which is several orders of magnitude smaller than for strongly decaying mesons of comparable mass i.e. for the  $\rho$  and  $\omega$ . This is evidence for the forbiddingness of the  $\eta$  decay into energetically accessible final states of neutral and charged pions. The decay  $\eta \rightarrow 3\pi$  does not obey  $G$  parity conservation nor isospin or charge symmetry; it is responsible for 32.5% (22.6%) of the  $\eta$  decay width through the neutral  $3\pi^0$  (charged  $\pi^0\pi^+\pi^-$ ) channel. It occurs, besides a negligible electromagnetic contribution of second order [1, 2], as a strong decay, whose chiral symmetry characteristics can be treated by introducing the *effective* Lagrangian of Chiral Perturbation Theory [3]. They lead to predictions of decay rates as a function of the quark mass difference ( $m_d - m_u$ ) that enters with the flavor symmetry breaking quark-mass term in the QCD Lagrangian [3, 4]. As a consequence, quantities that depend on the decay amplitude  $A(\eta \rightarrow 3\pi)$  give access to the mass difference ( $m_d - m_u$ ); among them are the decay widths  $\Gamma(\eta \rightarrow 3\pi)$ , the ratio  $R = \Gamma(\eta \rightarrow 3\pi^0)/\Gamma(\eta \rightarrow \pi^+\pi^-\pi^0)$ , and the distribution of the pions in the respective Dalitz plots.

In lowest order  $\chi PT$  one finds for the decay amplitude  $A(\eta \rightarrow 3\pi)$

$$A = \frac{1}{Q^2} \frac{m_K^2}{m_\pi^2} \frac{m_\pi^2 - m_K^2}{\sqrt{27}F_\pi^2} M(s, t, u) \quad (1)$$

<sup>1</sup>Presented at the Workshop on Production and Decay of  $\eta$  and  $\eta'$  Mesons (ETA05), Cracow, 15–18 September 2005.

<sup>2</sup>E-mail address: christian.pauly@desy.de

with the pion decay constant  $F_\pi$  and

$$\frac{1}{Q^2} = \frac{m_d^2 - m_u^2}{m_s^2 - \frac{1}{4}(m_d + m_u)^2}. \quad (2)$$

$M(s, t, u)$  is a dimensionless factor that involves exclusively measurable quantities. Having a good theoretical prediction for  $M$ , the quark mass ratio  $Q$  can be calculated from the decay rate  $\Gamma(\eta \rightarrow 3\pi) \propto A^2 \propto Q^{-4}$ .

The present work is primarily devoted to the investigation of the neutral decay  $\eta \rightarrow 3\pi^0$ . The expansion of the decay amplitude  $A$  around the center of the Dalitz plot yields [5]

$$A = 3c_0 \left[ 1 + 2\alpha \sum_{i=1}^3 \frac{(s_{\pi_i^0} - s_0)^2}{4m_\eta^2(m_\eta - 3m_{\pi_i^0})^2} \right] \quad (3)$$

with  $s_{\pi_i^0} = (p_\eta - p_{\pi_i^0})^2$  and  $s_0 = m_{\pi^0}^2 + \frac{1}{3}m_\eta^2$ , and an overall normalization constant  $c_0$ . This expression is symmetrized with respect to the three indistinguishable  $\pi^0$  in the final state. In lowest order of  $\chi PT$  the plot should be uniform. Deviations in the experimental Dalitz plot result from the energy dependent  $\pi^0\pi^0$  interaction. This is, however, a small effect. To make it visible, the experimental Dalitz plot is linearized by introducing the variable  $z$ :

$$z = \frac{6}{(m_\eta - 3m_{\pi^0})^2} \sum_{i=1}^3 \left(E_i - \frac{m_\eta}{3}\right)^2 = \frac{\rho^2}{\rho_{max}^2}, \quad (4)$$

where  $\rho$  is the distance from the center of the Dalitz plot. In ring intervals  $[\rho, \rho + \delta\rho]$  around this center the plot density should be constant. The coefficient  $\alpha$  is in terms of eq.(3)

$$|A|^2 \propto 1 + 2\alpha z \quad (5)$$

a measure of the nonuniformity.

The Dalitz plot study is preceded by a determination of the cross sections for the prompt  $pp \rightarrow pp3\pi^0$  and resonant  $pp \rightarrow pp(\eta \rightarrow 3\pi^0)$  process.

## 2 Measurement and data reduction

The presented analysis is based on data taken during two beamtimes in September and December 2003, using the WASA hydrogen pellet target system and a proton beam of 1360 MeV resp. 1450 MeV kinetic energy, corresponding to center of mass excess energies of 41 MeV and 75 MeV above the  $\eta$  production threshold.

In order to select the prompt and resonant  $3\pi^0$  production, all analyzed events are required to have two protons detected in the multilayered forward detector, and six gammas (from subsequent  $\pi^0 \rightarrow \gamma\gamma$  decays) being measured in the CsI calorimeter consisting of 1012 crystals (see [6] for a detailed description of the CELSIUS-WASA detector setup). The proton proton missing mass determination in the forward detector is used to separate the prompt and resonant production, without applying any further conditions on the decay system.

Strict time cuts as well as some additional kinematical cuts are applied to suppress background coming from overlapping events and from  $pp \rightarrow pp2\pi^0$  reactions with additional hits in

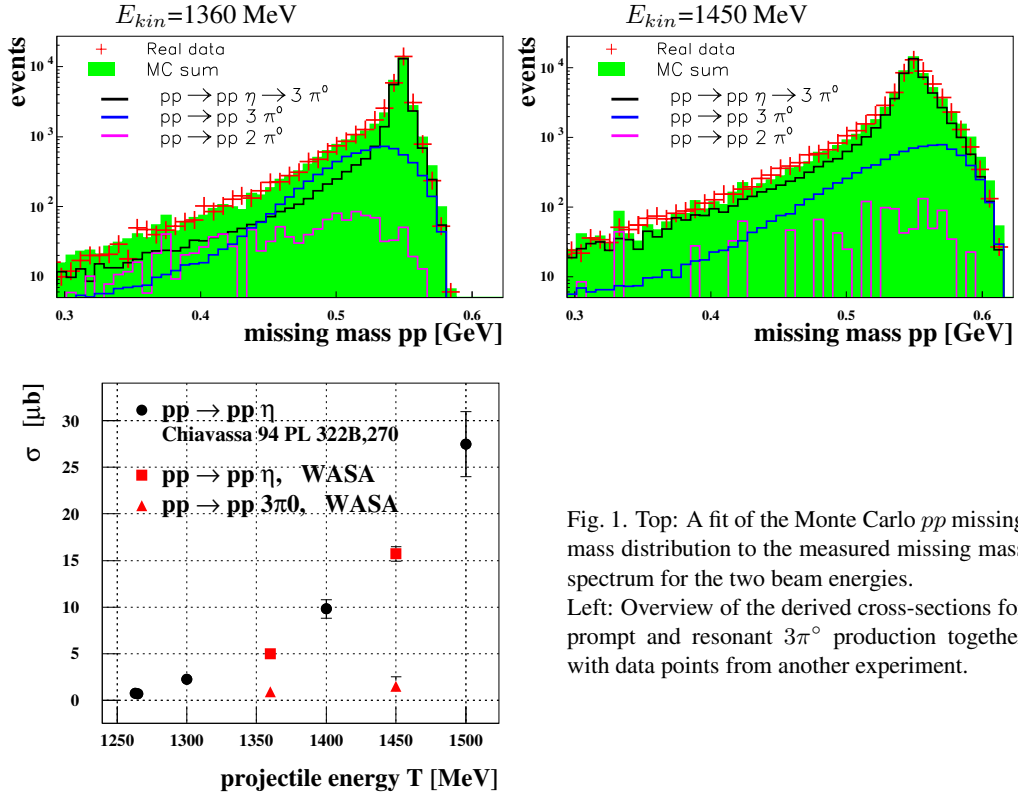


Fig. 1. Top: A fit of the Monte Carlo  $pp$  missing mass distribution to the measured missing mass spectrum for the two beam energies.

Left: Overview of the derived cross-sections for prompt and resonant  $3\pi^0$  production together with data points from another experiment.

the calorimeter due to hit cluster split-offs. The contribution of  $2\pi^0$  background to the data sample is very small, as it is seen from Monte Carlo simulations with the cross section fixed to  $200 \mu b$  (1360 MeV) resp.  $300 \mu b$  (1450 MeV), based on an earlier CELSIUS-WASA measurement.

All possible 15 combinations of the 6 reconstructed gammas to form 3 individual  $\pi^0 \rightarrow \gamma\gamma$  pairs are compared by means of a parameter  $\chi^2 = \sum_{i=1}^3 \frac{(IM(\gamma\gamma)_i - M_{\pi^0})^2}{\sigma_{Det}^2}$ , with  $IM(\gamma\gamma)_i$  being the invariant mass of the  $i^{th}$   $\gamma\gamma$  pair, and  $\sigma_{Det}$  being the detector invariant mass resolution.

The most probable (or the two most probable) combination is used for a final kinematical fit of the full event with 7 resp. 8 constraints: four-momentum conservation, 3 ( $\gamma\gamma \equiv \pi^0$ ) constraints, ( $6\gamma \equiv \eta$ ) constraint for the Dalitz plot. A cut on the  $\chi^2$  of the fit is applied which further suppresses the background. All distributions of kinematic variables are reproduced in the Monte Carlo simulation based on the following three reaction channels:  $pp \rightarrow pp(\eta \rightarrow 3\pi^0)$ ,  $pp \rightarrow pp3\pi^0$  and  $pp \rightarrow pp2\pi^0$ .

### 3 Cross section determination for prompt $3\pi^0$ production

Prompt  $3\pi^0$  production is one of the major background channels, not only for the  $\eta \rightarrow 3\pi^0$  decay, but also for several other  $\eta$  decay channels. Thus an exact knowledge of the cross section

is important. The simultaneous measurement of both prompt and resonant  $3\pi^0$  production in CELSIUS-WASA can be used to derive the cross section for the prompt  $3\pi^0$  production channel using the resonant  $\eta$  decay for normalization and for cross check of the measurement efficiency.

The  $\eta$ -peak clearly stands out in the proton proton missing mass distribution. A fit of the appropriate Monte Carlo contributions to the measured missing mass spectrum yields their relative weights, and together with the well known eta production cross section and branching ratio, the prompt  $3\pi^0$  cross section can be extracted without reference to any luminosity determination or detailed acceptance studies.

Fig.1 shows the result of the best fit for the two beam energies: 1360 and 1450 MeV. The resulting cross sections are  $\sigma_{pp \rightarrow pp3\pi^0}^{T=1360 \text{ MeV}} = 0.92 \pm 0.1 \mu\text{b}$  and  $\sigma_{pp \rightarrow pp3\pi^0}^{T=1450 \text{ MeV}} = 1.50_{-0.5}^{+1.0} \mu\text{b}$ , based on literature values for the  $\eta$  production cross section of  $5 \mu\text{b}$  resp.  $15 \mu\text{b}$  ([7], [8]) and a  $3\pi^0$  decay branching ratio of 32.51%.

Using the measured luminosity (from the concurrent  $pp$  elastic scattering) we can also extract the  $\eta$ -production cross section from the number of  $pp \rightarrow pp\eta$  events given by the fit, resulting in  $\sigma_{pp \rightarrow pp\eta}^{T=1360 \text{ MeV}} = 5.0 \pm 0.3 \mu\text{b}$  and  $\sigma_{pp \rightarrow pp\eta}^{T=1450 \text{ MeV}} = 15.7 \pm 0.8 \mu\text{b}$ , with errors based on an uncertainty in the luminosity determination of 5 %. The good agreement shows that the detector- and trigger acceptance are well understood.

A similar approach is used to deduce an upper limit for prompt  $4\pi^0$  production at 1450 MeV, yielding  $\sigma_{pp \rightarrow pp4\pi^0}^{T=1450 \text{ MeV}} \leq 0.01 \mu\text{b}$ . The lower part of Fig. 1 shows an overview of the CELSIUS-WASA results for  $3\pi^0$  production cross sections together with results from [7].

#### 4 Dalitz plot and slope parameter $\alpha$

To obtain the symmetrized Dalitz plot of the  $3\pi^0$  from the  $\eta$  decay, a narrow band around the  $\eta$  mass of the proton proton missing mass spectrum is selected to reduce the background from prompt  $3\pi^0$  production. The remaining background contribution is in the order of 5 % and assumed to be phase space distributed. The resulting Dalitz plot and radial density distribution  $z$  (eq. 4) are shown in the left part of fig. 2, separately for Monte Carlo and real data. The deviation from a circular shape of the Dalitz plot is due to the relativistic kinematics. The Monte Carlo simulation is based on pure phase space hence the resulting Monte Carlo plot reflects the detector acceptance. The acceptance corrected density distribution, as shown in the right part of fig.2, is obtained as the ratio of real and Monte Carlo simulated events. The real data sample consists of ca. 80.000 events after all cuts. A linear fit yields the result for the slope parameter  $\alpha$  (eq. 5) with  $\alpha = -0.027 \pm 0.009(\text{stat}) \pm 0.01(\text{syst})$ . For our present result, we excluded the first and the last three bins due to low statistics or systematic uncertainties.

The systematic error was obtained by variation of all essential cuts applied in the reconstruction: we varied the  $\chi^2$  cut of the kinematical fit, the combinatorical purity of the sample, the missing mass cut, the fit region, and we selected different data subsamples.

The result, at present limited by the available statistics, is within errors compatible with both the results from Crystal Ball ( $\alpha = -0.031(4)$ , based on  $10^6$  events, [9]) as well as the recent KLOE result ( $\alpha = -0.013 \pm 0.005(\text{stat}) \pm 0.004(\text{syst})$ , [10]). We hope for further improvement by including recent data periods with deuteron target into the analysis.

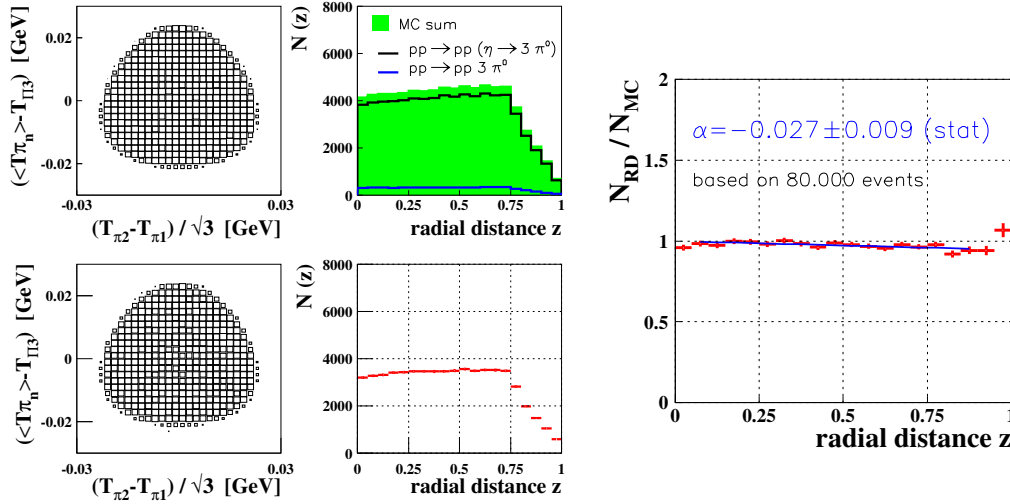


Fig. 2. Dalitz plot and radial density distribution for Monte Carlo (left, upper part) and real data (left, lower part). The right part shows the acceptance corrected Dalitz plot density distribution together with a linear fit to obtain the slope parameter  $\alpha$ .

**Acknowledgement:** The CELSIUS-WASA collaboration gratefully acknowledges the great support received from the CELSIUS accelerator group, and the financial support by the BMBF, Contract 06HH152.

#### References

- [1] A. V. Anisovich, H. Leutwyler: *Phys. Lett. B* **375** (1996) 335
- [2] N. Beisert, B. Borasoy: *arXiv:hep-ph/0301058*
- [3] J. Bijnens, J. Gasser: *Phys. Scripta T* **99** (2002) 34
- [4] B. M. M. K. Nefkens, J. W. Price: *Phys. Scripta T* **99** (2002) 114
- [5] J. Gasser, H. Leutwyler: *Nucl. Phys. B* **250** (1985) 539
- [6] J. Zabierowski et al.: *Phys. Scr. T* **99** (2002) 159
- [7] E. Chiavassa et al.: *Phys. Lett. B* **322** (1994) 270
- [8] H. Calén et al.: *Phys. Lett. B* **366** (1996) 39
- [9] W. B. Tippens et al.: *Phys. Rev. Lett.* **87**(2001) 1920011
- [10] F. Ambrosino et al.: *arXiv:hep-ex/0505074*